Journal of Carcinogenesis
Covering Genesis to Therapeutics

Journal of Carcinogenesis, ISSN: 1477-3163
2025; Vol 24: Issue 9s, https://carcinogenesis.com/

Eco-Friendly Fabrication of Silver Sulphide Nanostructures via Microwave Irradiation: Structural Characterization and Pharmacologically Relevant Cytotoxicity Studies

Richa Kothari[1*], Manoj Kumar Bajhaiya[2], Vivek Tripathi[1]

[1]School of Sciences, ITM University, Gwalior (M.P.), India -474011

[2]School of Pharmacy, ITM University, Gwalior (M.P.), India -474011

Corresponding: richakothari@itmuniversity.ac.in

ABSTRACT

In this study, we present a rapid, template -free, and environmentally benign synthetic strategy for the fabrication of structurally diverse silver sulphide (Ag2S) nano structures under ambident conditions. This synthesis is based on a microwave assisted thermal decomposition of a macrocyclic ligand -coordinated silver (I) complex employed as a single-source molecular precursor. This ecofriendly method enables the synthesis of silver sulphide nanostructures with different morphologies, including nano spheres and nanotubes, composed primarily of assembled nano plates and nanoparticles. Synthetic parameters-precursor stoichiometry, and the nature of counterions -revealed that ionic species significantly influence the resultant morphology specifically sulphate, nitrate, bromide, hydroxide ions favoured the formation of tubular nanostructures, whereas chloride ions predominantly yielded spherical architectures. The resulting ecofriendly nanomaterials were extensively characterized using elemental analysis, Fourier -transform infrared spectroscopy (FT-IR),UV-Vis spectroscopy (UV-Vis), thermogravimetric analysis (TGA),X-ray diffraction(XRD),transmission electron microscopy(TEM),and scanning electron microscopy(SEM).FT-IR spectral data indicated notable shifts in vibrational bands, in silver (I) complex, affirming successful coordination of the ligand to the silver ion in +1 oxidation state. XRD confirmed the crystalline phase purity of silver sulphide nanostructures, while SEM revealed monodisperse spherical particles averaging ~ 78 nm in diameter. A prominent absorption peaks at 353 & 378 nm in UV spectrum further corroborated the optical and nano scale features of the synthesized particles. SEM analysis displayed agglomerated, grain-like surface textures characteristic of Ag2S nano structures. The incorporation of non-polar solvents like DMSO (dimethyl sulfoxide) under microwave irradiation was found to significantly enhance reaction kinetics, reduce by-products of reaction and improve the overall quality of the nanomaterials. In addition to structural and optical characterization, the bioactive potential of the synthesised silver sulphide nano particles was evaluated. The materials exhibited notable pharmacological properties, including anticancer, antioxidant, and anti-inflammatory activities likely arising from the electronic characteristics of the substituent groups on the molecular precursor. Furthermore, cytotoxic assays against MCF -7 breast cancer cell lines, revealed significant biological activity, under scoring the therapeutic promise of the nano structures. This ecofriendly, microwave-assisted route represents a robust and efficient methodology for producing bio-functional Ag2S nanostructures, holding great potential for future applications in biomedicine, particularly in cancer therapy and molecular diagnostics.

KEYWORDS: *Silver sulphide nano particles, Single source molecular precursor, Microwave -assisted synthesis, biological activity*

How to Cite: Richa Kothari, Manoj Kumar Bajhaiya, Vivek Tripathi., (2025) Eco-Friendly Fabrication of Silver Sulphide Nanostructures via Microwave Irradiation: Structural Characterization and Pharmacologically Relevant Cytotoxicity Studies, *Journal of Carcinogenesis*, *Vol.24, No.9s*, 1-18.

1. INTRODUCTION

Silver nanoparticles (AgNP's) have garnered significant attention in recent years due to their remarkable physicochemical properties and broad spectrum of potential applications. Their distinctive optical, electrical, thermal, and biological characteristics -such as high electrical conductivity, antimicrobial efficacy, and catalytic activity -make them valuable in a wide array of fields including medicine, food safety, health care, consumer goods, and industrial processes.[1-3]These nanomaterials have been extensively utilised as antibacterial agents, in wound dressing, medical device coating ,optical sensors, cosmetics, and even in drug delivery systems and cancer therapy, where they have been shown to enhance the efficacy of anticancer drugs.[4-6]The unique behaviour of AgNP's can be largely attributed to their nano scale dimensions and high surface-to volume ration, which significantly influence their physical, chemical and biological interactions[7-8].To meet the increasing demand for these nanoparticles, a variety of synthetic procedures have been developed. Traditional physical and chemical approaches, although effective, often involve high costs and environmental hazards [1,9]. In contrast, biological or "green" synthetic methods have emerged as promising alternatives. These eco-friendly techniques offer several advantages, including simplicity, cost-effectiveness, and the ability to produce nanoparticles with controlled size and morphology, often with enhanced stability and biocompatibility [1]. Following synthesis, thorough characterization of silver nanoparticles is critical to ensure their safety and efficacy for biomedical applications. The biological behaviour of nano particles such as toxicity, cellular uptake, and therapeutic activity is largely influenced by their physico chemical properties, including size, shape, surface chemistry, solubility and aggregation state.[10-12].Comprehensive characterization is typically carried out using a suite of analytical techniques such as UV-Visible spectroscopy-ray diffraction (XRD),Fourier -transform spectroscopy(FT-IR),Transmission electron microscopy (TEM) &Scanning electron microscopy(SEM).Notably, the biological activity of silver nanoparticles is highly dependent on several factors, particle size & shape, surface modification, dissolution behaviour ,ion release kinetics and the nature of the reducing and capping agents used in synthesis{15].These factors collectively influence not only cytotoxicity but also the pharmacokinetics and biodistribution of therapeutic agents, enhancing their bioavailability and therapeutic outcomes after both local and systemic administration [16-19].Thus, the design and development of AgNP's with uniform ,well -defined physicochemical properties is essential for their successful application in modern medicines[20-24].

Cancer a multifaceted and globally prevalent disease, is characterized by uncontrolled cell proliferation influenced by genetic, environmental, and life style factors [25]. Standard cancer treatment modalities-such as chemotherapy, radiotherapy, surgery, immunotherapy, -are often limited by toxicity and non-specificity. In this context, AgNP's have emerged as promising candidates due to their anticancer, anti-angiogenic, and diagnostic capabilities. Given their potential, there is an urgent need to better understand and optimize their synthesis, characterization, and application in oncology. This study aims to consolidate recent advancements in the green synthesis, structural and functional characterization, and biomedical applications of AgNP's, with a particular focus on their anti-inflammatory and anticancer properties.

2. EXPERIMENTAL

2.1 Materials & Methods

All chemicals used were of analytical grade. Silver nitrate (99.8% pure), curcumin and thiosemicarbazide hydrochloride, DPPH, & BSA were purchase from Merk company Pvt. Ltd Bengaluru, India. All the chemicals used as received without further purification. Distilled water was used for all the experiments conducted in our study.

2.2 Instrumentation

Ultrasonicator, microwave, water bath, deep fridger, cooling centrifuge, mechanical stirrer, UV -Vis spectrophotometer

2.3 Spectroscopic Characterization of compounds

Elemental analyses of silver (I) complex were determined in the microanalytical unit using CHN elemental analyzer. Perkin Elmer 2400 from CDRI ,Lucknow U.P. FT-IR spectra of synthesised compounds were recorded on a Perkin Elmer FT-IR spectrophotometer in PC Ray research center, ITM University, Gwalior-Vis spetra of compounds were recorded on Perkin Elmer UV -vis lambda 25 in PC ray research center, ITM University ,Gwalior of silver nanoparticles were carried out at room temperature using a Bruker axis D $_8$ using Cuα radiations(1.54 A^0) over a 2θ collection range of 20 -80 ^{0} from CIF, Jiwaji University, Gwalior and molar conductance of silver complex was monitored by using a Digital conductivity meter in DMSO solvent (1X10^{-3} M) .All chemical reactions were monitored by TLC using under UV lamp .IUPAC nomenclature and calculation of molecular weight of complex was performed by Chem Bio Draw 12 software.

2.4 Synthesis of Macrocyclic Ligand

The curcumin was obtained from Sigma Aldrich and thiosemicarbazide hydrochloride in glacial acetic acid as starting material [17]. Ligand was prepared by the reaction of curcumin with thiosemicarbazide in them molar ratio 1:1 using anhydrous methanol as a solvent.The liquid was obtained upon refluxing the reaction mixture of curcumin and thiosemicarbazide for 6 hours at 80^{0}C.

Curcumin (99% Pure) + Thiosemicarbazide hydrochloride → Ligand(L)
Colour: Off white crystals from ethanol, yield: 60%. m.pt.-, H ^{1}NMR (500MH$_Z$,DMSO-d$_6$) δ ppm:1.34 (9H,CH$_3$),1.42s (9H,3 CH$_3$,6.7 s (1H,CH$_{Ar}$),7.10(1H,OH),8.74s(1H,CH=N)13.19s (1H,SH); FT-IR (ϑ,cm^{-1}); 3344 (s), $\vartheta_{(O-H)}$ *;1616(s0*

$\vartheta(C=N); 1166m, \vartheta$
$(C-O)-1114, \vartheta(C(aromatic-N)1274\,m, \vartheta(S-H)2578(w), \vartheta(C-S), 688\,w$
UV-Vis: λ, nm:320(4.26),378(4.30),413(3.62), Mass Spectrum, m/z:863.96[M^+] [$C_{24}H_{31}O_5N_3S$]

2.4 Synthesis of Silver (I) Complex from Macrocyclic Ligand

In the present study, silver (I) complex was synthesised employing a refluxing approach, a well -established methodology in coordination chemistry. In this involves the in-situ construction of ligand under the direction of a central metal ion, which acts as a structural scaffold to guide the spatial arrangement of donor atoms for effective coordination. Stoichiometric amounts of ligand and silver nitrate (2:1) molar ratio were reacted in methanol. The reaction mixture was subjected to reflux under constant stirring for 8 hours, facilitating the formation of a ligand framework coordinated around the silver center. The appearance of black precipitate upon completion of the reflux period was indicative of successful complex formation. After completion of reaction, the solvent was removed under reduced pressure, and the residue was treated with ethanol to terminate the reaction and facilitates the precipitation of Silver (I) complex. The solid product was isolated by filtration, thoroughly washed with cold ethanol to eliminate unreacted starting materials and by products and dried over anhydrous calcium chloride in a desiccator. The final silver complex was obtained in a good yield,and its purity was confirmed via thin layer chromatography (TLC0 and elemental analysis. These results collectively validate the efficiency of the refluxing method in constructing stable macrocyclic architectures with potential medicinal applications in coordination and bioinorganic chemistry.

Colour - Black crystals from ethanol, yield: 85%. m.pt.-,
Anal.Calcd. for [$C_{45}H_{22}O_{10}N_6S_2Ag$]; C,43.26; H,4.68;Ag 22.80;N,8.92;S,13.26;
mFound: C,43.18;H,4.36;Ag,22.82,N,8.82;S,13.20; H ^{1}NMR (500MH$_Z$,DMSO-d_6) δ ppm:1.36 (9H,CH_3),1.42s (9H,3 CH_3,6.7 s (1H,CH_{Ar}),7.10(1H,OH),8.74s(1H,CH=N)13.19s (1H,SH); FT-IR (ϑ,cm^{-1}); 3312 (s), $\vartheta_{(O-H)}$;1651(s) $\vartheta(C=N); 1186m, \vartheta(C-O)-1272, \vartheta(C(aromatic-N)1284\,m, \vartheta(S-H)2612(w), \vartheta(C-S), 673\,w$
UV-Vis: λ, nm:378(4.30),413(3.62), Molar conductance: 18 ohm $^{-1}$ cm ^{2} mol $^{-1}$ Mass Spectrum, m/z:978 amu [$C_{45}H_{22}O_{10}N_6S_2Ag$]

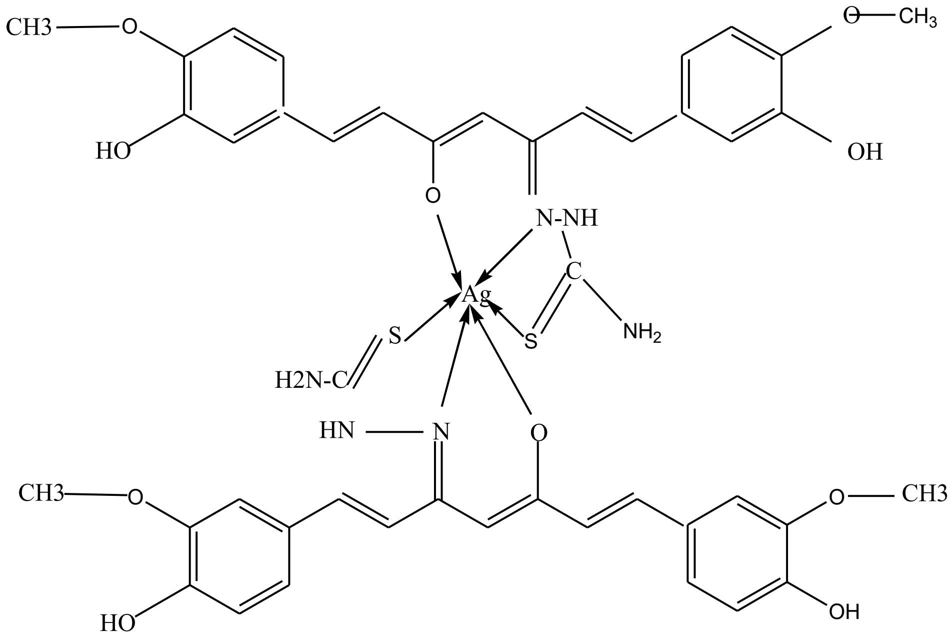

Figure -1 Synthesis of Silver (I) Complex from Macrocyclic Ligand

2.5 Microwave -Assisted Conversion of Ag(I) complex into silver nanoparticles

Silver nanoparticles (AgNP's) were synthesised from a pre-formed macrocyclic Ag(I) complex through a combined solvent -mediated Sono chemical, and microwave -assisted approach. Precisely,1 g of the synthesized Ag(I) complex was weighted and dissolved in 50 ml of DMSO (dimethyl sulfoxide) solvent in 100 ml round – bottom flask to serve as the reaction medium to achieve homogenous dispersion and facilitate molecular recognition, the resulting solution underwent ultrasonic irradiation using a piezo electric sandwich-type transducer operating at a resonant frequency of 40 kHz. The sonication process was conducted for 30 minutes at a constant temperature at 75^{0}C, uniform mixing and potentially aiding ligand exchange or realignment within coordination environment. After sonication process, the reaction mixture was allowed to age undisturbed for an additional 30 minutes to encourage nucleation and the pre-organised of reactive species. Subsequently, the mixture was subjected to microwave irradiation in a conventional microwave over operating at 800W for 15 minutes. The rapid increase in temperature and internal pressure under microwave conditions facilitated the swift decomposition of the silver complex and conversion into silver nanoparticles as evidence by an immediate visual colour change in the reaction mixture. After the completion of microwave treatment, the mixture was allowed to cool to room temperature. The resulting colloidal suspension was allowed to separate the solid silver nanoparticles, which were then washed repeatedly with ethanol and distilled water to remove residual solvents and unreacted precursors. The purified nanoparticles were subsequently dried over vacuum physio-chemical and structural for further characterization.

Figure -2 Microwave -assisted synthesis of silver nanoparticles from Silver (I) complex

2.6 In-vitro anti- oxidant activity of synthesised compounds

The anti-oxidant potential of synthesised compounds was assessed using the DPPH (2,2-diphenyl -1-picrylhydrazyl) radical scavenging assay, in accordance with the method described by Hataro et al., with minor modifications. Ascorbic acid served as the reference antioxidant standard for comparative analysis. A 0.04% w/v DPPH stock solution was freshly prepared in methanol. For the assay,1.0 ml of the DPPH solution (appro.0.3 mmol) was added to 3.0 ml of the test compound solution at varying concentrations (20,40,60,80& 100µg/ml) A blank sample was prepared by mixing 3.0ml of test compound solution with 1.0 ml of methanol, except DPPH reagent. The negative control consisted of 1.0 ml of DPPH solution & 3.0 ml DMSO, solvent used for dissolving the test compounds. All mixtures were incubated at room temperature(25 ± 2^0C) in the dark for 30 minutes to minimise potential photo-induced degradation of the DPPH radical. Post-incubation, the absorbance of each reaction mixture was measured at 517 nm wavelength using a UV-Visible spectrophotometer. A decrease in absorbance indicated the free radical scavenging capacity of test compounds. The percentage of DPPH radical scavenging activity (% RSA) was calculated using following equation:

Radical Scavenging Activity (%) = [Absorbance $_{(Control)}$ – Absorbance$_{(sample)]}$ /Absorbance $_{(Control)\ X\ 100}$

Where,

Absorbance $_{(Control)}$ = Absorbance of DPPH solution without test sample (negative control)
Absorbance$_{(sample)]}$ = Absorbance of DPPH solution in the presence of synthesized compound
Each experiment was conducted was conducted in triplicate, and the results are presented as mean± standard deviation to ensure reliability and statistical significance. The results provide qualitative insight into the antioxidant efficacy of synthesised compounds, which may be attributed to their potential electron or hydrogen donating capabilities.

2.7 Invitro Anti-inflammatory activity of compounds via inhibition of albumin denaturation

This activity was assessed invitro by evaluating their ability to inhibit heat- induced denaturation of bovine serum albumin (BSA). Protein denaturation, a process commonly associated with the onset of inflammatory responses, serves as biological marker for screening anti-inflammatory agents. Substances that prevent thermal denaturation of proteins are thus considered to possess anti-inflammatory activity; as they contribute to maintaining the functional integrity of cellular proteins under stress conditions. The assay was conducted by preparing reaction mixtures containing 0.45ml of a 3% aqueous solution of BSA and 0.05% of synthesised compound solutions at varying concentrations (10,20,30,40 & 50µg/ml), resulting in a final volume of 05 ml per compound. The p^H of each reaction mixture was carefully adjusted to 6.3 using a minimal volume of 1N hydrochloric acid to maintain near-physiological conditions favourable for protein stasbility. Synthesised compounds were pre-incubated at 37 ± 0.5^0C for 20 minutes for facilitate potential interactions between the compounds and the protein substrate. This was followed by exposure to thermal stress at 80±0.5^{0}C for 20 minutes, promoting protein denaturation process. After thermal treatment, all reaction mixtures of compounds were cooled at room temperature, and the absorbance of each compound was recorded at 660 nm using UV- Visible spectrophotometer. In this experiment. Diclofenac sodium, a standard non-steroidal anti-inflammatory drug (NSAID), was used as the positive control under identical conditions. A negative control (BSA without synthesised compound) was also included. The percentage inhibition of protein denaturation was calculated using the following formula:

Percent Inhibition (%)= [$Abs_{(control)}$-$Abs_{(sample)}$/ $Abs_{(control)}$]X 100
Where ; $Abs_{(control)}$ = Absorbance of BSA solution without test sample.
$Abs_{(sample)}$= Absorbance of BSA solution in the presence of synthesised compound.

All experiments were performed in triplicate, and the results are presented as mean± standard deviation (SD) to ensure statistical reliability. This assay provides an effective and biologically relevant model for evaluating the anti-denaturant and anti-inflammatory efficacy of novel compounds through their capacity to stabilize protein conformation under thermal stress, thereby mimicking physiological inflammatory conditions.

2.8 Evaluation of Anti-Proliferative Activity of Synthesized Molecules
2.8.1 Preparation of Samples for Cytotoxicity Evaluation-
To evaluate the cytotoxic potential of the synthesised compounds, precisely 10 mg of each compound -silver(I) complex and silver nanoparticles -was weighed using an analytical balance and dissolved in minimum essential medium (MEM) supplemented with 2% heat-inactivated fetal bovine serum. This resulted in a primary stock solution at a concentration of 10 mg/ml. The stock solutions were subsequently sterilized using 0.45 µm syringe filters and subjected to a series of two -fold serial dilutions to prepare working solutions of lower concentrations for cytotoxic assessment of synthesised compounds.

2.8.2 Cell Line and Culture Conditions
Human breast cancer adenocarcinoma cells (MCF-7) were procured from the National centre for cell science (NCCS) Pune, India. The cells were cultured in Roswell Park Memorial Institute (RPMI)-1640 medium supplemented with 10% (v/v) FBS,100µg/ml penicillin, 100µg/ml streptomycin Cells were maintained under standard incubation 37±0.5^{0}C in a humidified atmosphere containing 5% CO_2 and 95% air. Sub-culturing was performed upon reaching 70-80% confluency using 0.25% trypsin -EDTA solution.

2.8.3 Cytotoxicity Assessment via MTT assay
The cytotoxic effects of the synthesised silver (I) complex and silver nanoparticles were quantified using the MTT [3-(4,5-dimethylthiazol-2-yl)-2,5-diphenyltetrazolium bromide] colorimetric assay. This assay evaluates cellular metabolic activity as an indirect measure of cell viability bases on the reduction of MTT by mitochondrial dehydrogenase enzymes to an insoluble purple formazan product in viable cells.MCF-7 cells were seeded in 96 -well .The microtiter plates at a density of 1X 10^4 cells/well in 100µl of complete culture medium. After 24 hours of incubation to ensure cell adherence, the culture medium was replaced with 100µl of fresh medium containing varying concentrations of the synthesised compounds (1.56,3.125,6.25,12.5,25,50 and 100 µg/ml). The plates were then incubated for an additional 24 hours under standard culture conditions. After treatment period,10µl of MTT solution (5mg/ml in phosphate -buffer saline) was added to each well and incubated for 4 hours. The medium was then carefully removed, and the resulting formazan crystals were solubilized in 100µl of DMSO (dimethyl sulfoxide). Absorbance was recorded at 570 nm using a microplate spectrophotometer. The absorbance values obtained for synthesised compounds are directly proportional to the number of viable cells, allowing for the quantitative assessment of cytotoxicity of compounds.

2.8.4 Cell Viability and cytotoxic response
To establish a benchmark for cytotoxic efficacy,5 -Fluorouracil (5-FU),a well -characterized antineoplastic agent, was employed as the positive control across a concentration gradient ranging from 7.8µM to 1000 µM. Untreated MCF-7 cells cultured under identical conditions served as the negative control, representing base line cellular viability. All experimental conditions, including treatment and controls, were conducted in triplicate to ensure reproducibility and enable statistically robust analysis. Cell viability and cytotoxic response were quantified based on absorbance values obtained from the MTT assay using the following equation-

Cell viability (%) = [Absorbance $_{(sample)}$/Absorbance of $_{(control)}$]x 100
Cytotoxicity (%) = 100- Cell viability (%)
Whereas;
Abs $_{(sample)}$=represents the absorbance measured in wells containing cells treated with the synthesized compounds or 5 -FU.
$Abs_{(control)}$= denotes the absorbance from the untreated control cells

These calculations facilitated comparative assessment of synthesised compounds relative to the standard cytotoxic profile of 5-FU and the baseline established by the untreated control groups.

3. RESULTS & DISCUSSION

3.1 Physicochemical Characterization of compounds

The curcumin -thiosemicarbazide based ligand was synthesised via a condensation reaction between a primary amine and an aldehyde functional group, yielding the corresponding ligand. The silver (I) complex of this ligand was subsequently isolate from a mixed solvent system comprising acetone and acetonitrile, resulting in an amorphous or poorly crystalline solid. The complex exhibited poor solubility in non- polar organic solvents, limited solubility in acetonitrile, and appreciable solubility in polar aprotic solvents such as dimethyl formamide (DMF) and dimethyl sulfoxide (DMSO).

Molar conductivity measurements of synthesized silver complex in DMSO revealed value of 10 5 `$\Omega^{-1}cm^2mol^{-1}$, which are indicative of non-electrolytic behaviour. The conductivity value is consistent with the formation of neutral silver -ligand complex, suggesting the absence of significant ionic dissociation in the solution [26].

Table -1 Physico- chemical properties of synthesized compounds

S.N.	Colour	Melting point	yield	Molar conductance	Texture	solubility
Ligand	yellow	98	78	-	Light yellow precipitate	DMSO, DMF, Ethanol
Silver (I) complex	Green	105	76	105	Black crystalline powder	DMSO, DMF, Ethanol
Microwave-assisted Silver nanoparticles	Black	-	75	-	Crystalline material	DMSO & DMF

3.2 H¹NMR Spectroscopic Analysis of compounds

The structural characteristics and coordination behaviour of the synthesized ligand and its corresponding silver (I) complex were investigated using proton nuclear magnetic resonance spectroscopy in DMSO-d_6. The spectra of the free ligand exhibited characteristic features consistent with the proposed Schiff base structure. Two distinct singlets observed in the downfield region (δ=7.10-8.34ppm) and (δ=14.80 -15.24ppm) were assigned to the phenolic protons of the aromatic moiety ,with the intense de-shielding of the latter indicative of strong intramolecular hydrogen bonding .The aromatic protons of the aromatic ring appeared as singlets centred around δ≈6.7 ppm .The successful formation of the ligand was further corroborated by the appearance of singlet signals in the region $\delta = 8.74 - 9.30\ ppm, attri$buted to the azomethine (-CH=N-) protons. In addition, the presence of singlets at δ=5.64,5.70, & 13.19 ppm corresponding to thiol(-SH) protons provided further evidence of the thiosemicarbazide functionality. Upon complexation with silver centre, the H^1NMR spectra of complex revealed notable spectral changes. The complete disappearance of the -SH proton signals in silver complex is indicative of deprotonation and subsequent coordination of the thiol group to the silver ion. In Ag (I) complex, the azomethine nitrogen signal underwent a downfield shift to δ=9.18 ppm, suggesting its direct involvement in coordination with silver centre. Additionally, phenolic -OH signals exhibited minor shifts in silver (I) complex, which may reflect either coordination of hydroxyl groups to the metal centre or a disruption of intramolecular hydrogen bonding networks present in the free ligands. In some cases, the perturbation could also be attributed to the formation of new hydrogen bonding interactions involving uncoordinated hydroxyl functionalities within the complex. These spectral observations collectively support the selective and variable involvement of donor groups-thiol, azomethine, and hydroxyl-in the coordination chemistry of silver (I) complex, depending upon the ligand framework and local environment.

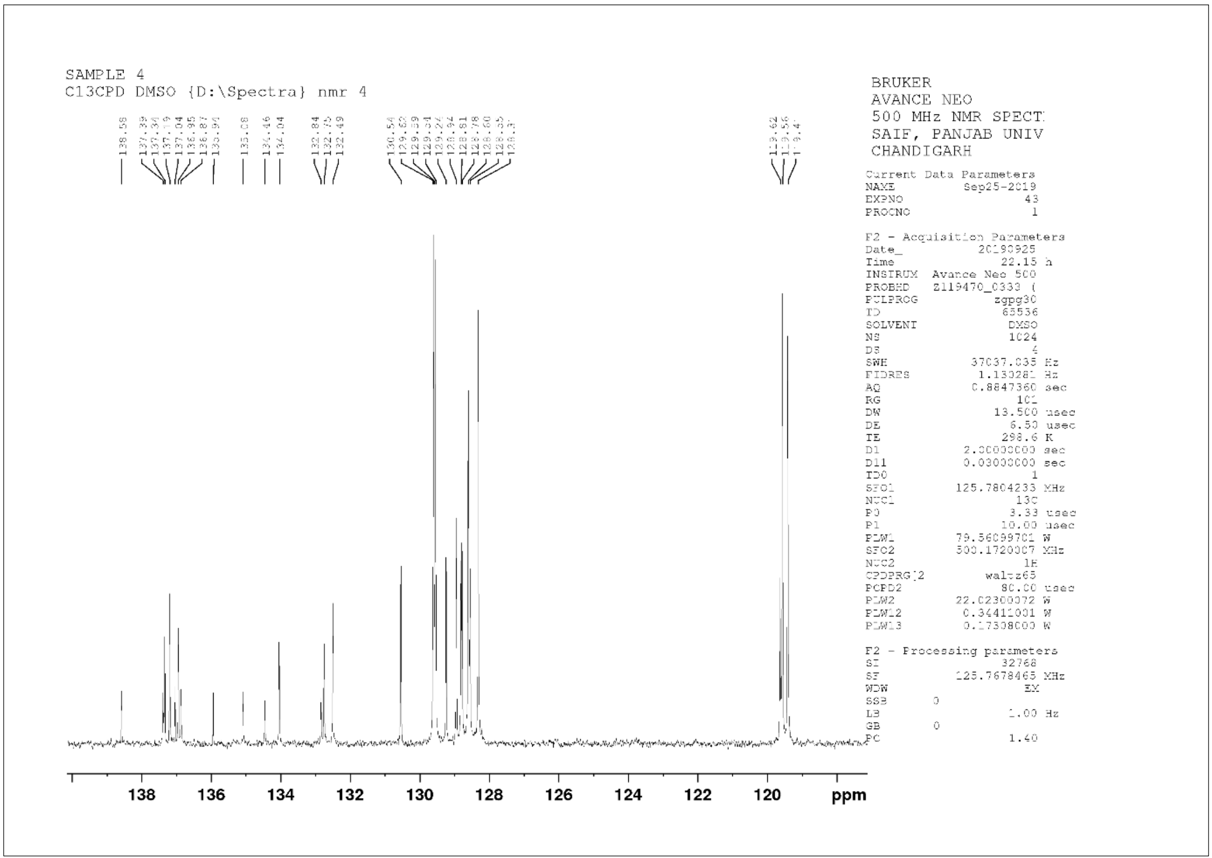

Figure -3 H[1]NMR spectra of Silver (I) complex

3.3 Spectroscopic Characterization & Coordination analysis
3.3.1 FT-IR analysis

Fourier -transform infrared spectroscopy (FT-IR) was employed to elucidate the coordination behaviour of the ligand and its corresponding Ag(I) complex. Comparative analysis of the spectra of ligand allowed for the identification of donor

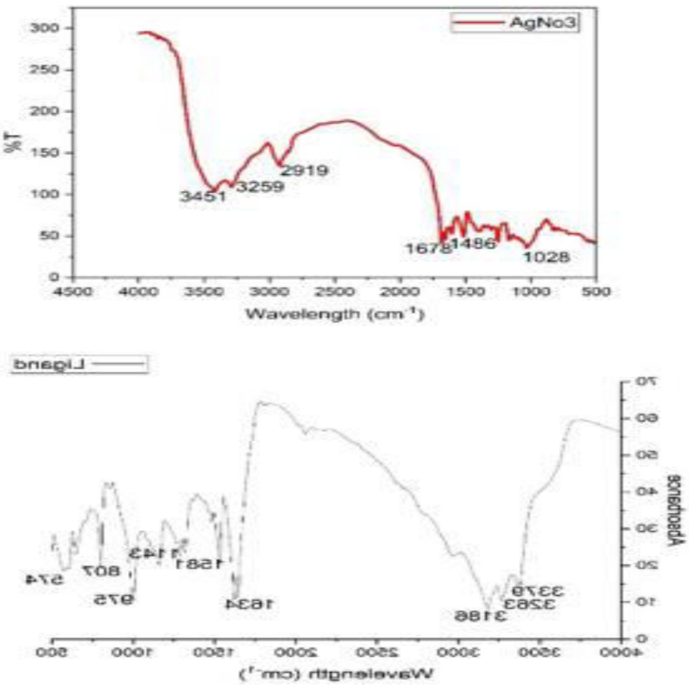

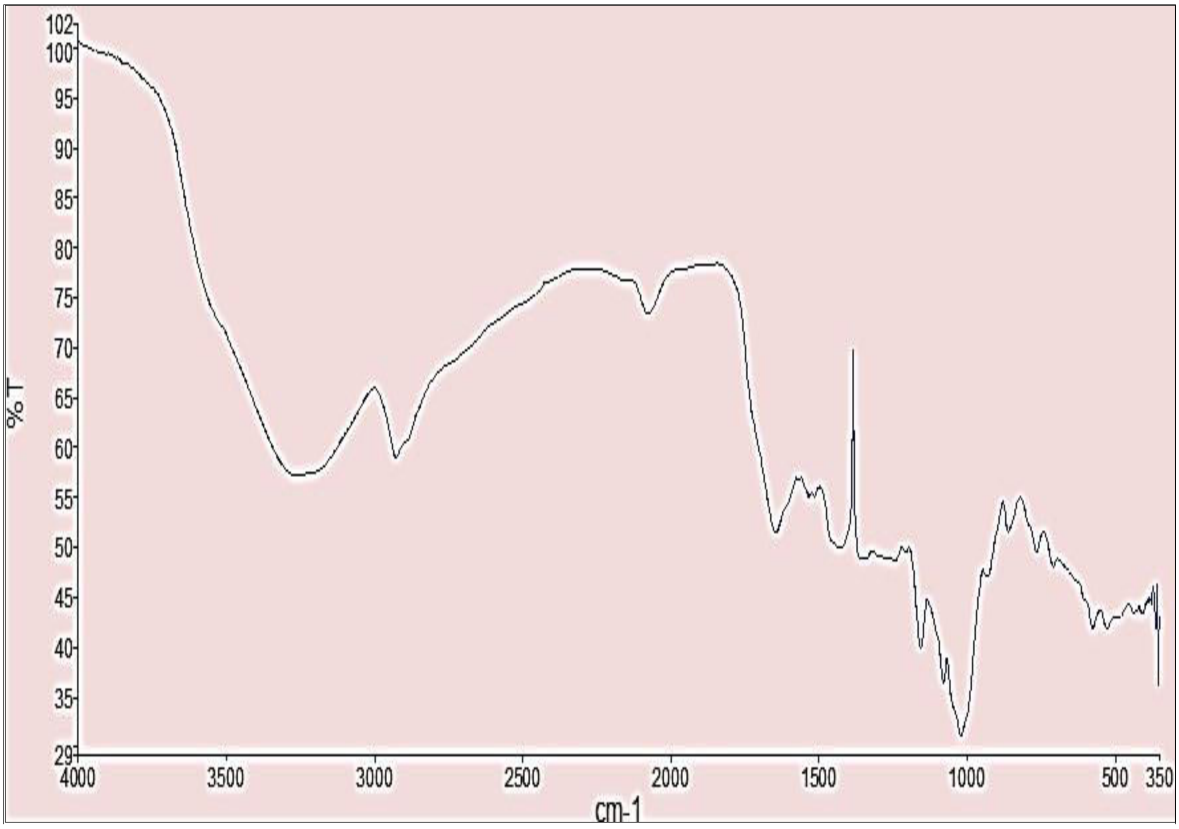

Figure -4 FT-IR Spectra of ligand,silver (I) complex and silver nanoparticles

atoms involved in coordination. In the spectra of the ligand, characteristic bands associated with non- coordinating moieties, such as aromatic C=C stretching of the benzene ring, remained unchanged in the corresponding complexes, suggesting these groups do not participate in the metal binding [26,27]. Importantly the absorption of absorption bands, typically attributed to thiosemicarbazone structures [27] indicates the absence of oxidized thiosemicarbazone ligand within the coordination sphere of silver complex. The broad O-H stretching bands observed in the range of 3396- 3342 cm^{-1} in the ligand spectra were blue shifted in the silver (I) complex, suggesting no direct coordination of phenolic oxygen to Ag centre. This interpretation is further supported by the unchanged C-O stretching region(1220-1400cm^{-1}), consistent with lack of metal -oxygen bond formation. In contrast, shifts in the azomethine C=N stretching vibrations (1650-1616 cm^{-1}) in the spectra of silver complex, indicate coordination through the imine nitrogen. This is further substantiated by the appearance of new bands in the 500-600 cm^{-1} region, which are typically associated with the metal -nitrogen (Ag-N) stretching mode

The weak S-H stretching bands present at 2600-2500 cm^{-1} in the free ligand is absent in the spectra of silver complex,indicating deprotonation and coordination of sulphur in the thiolate form. Silver complex uniquely exhibits a strong band at 1074 cm^{-1} consistent with coordination via both thiolate and thione (C=S) forms. Furthermore, a red shift of the -C-S- vibrations in complex (originally 630-600cm^{-1} in ligand) suggests involvement of the sulphur atom from the heterocyclic ring in metal coordination.

3.3.2 UV -Vis Spectroscopic Analysis

The UV-Vis absorption spectra of the ligand displayed high -energy bands in the 320-413 nm region, attributed to $\pi - \pi *$ $transitions$ of aromatic systems.{39]. Additional strong absorption bands in the range of 289-370nm corresponds to $\pi - \pi *$and n- $\pi *$*transitions of the azomethine moiety. In Ag (I) complex bathochromic shits of these bands to 413-420nm indicate electronic perturbation upon metal coordination, particularly involving the azomethine group. In the spectrum of silver complex, however largely shifted, reinforcing the IR-based conclusion that the imine group is involved in the coordination with silver centre.*

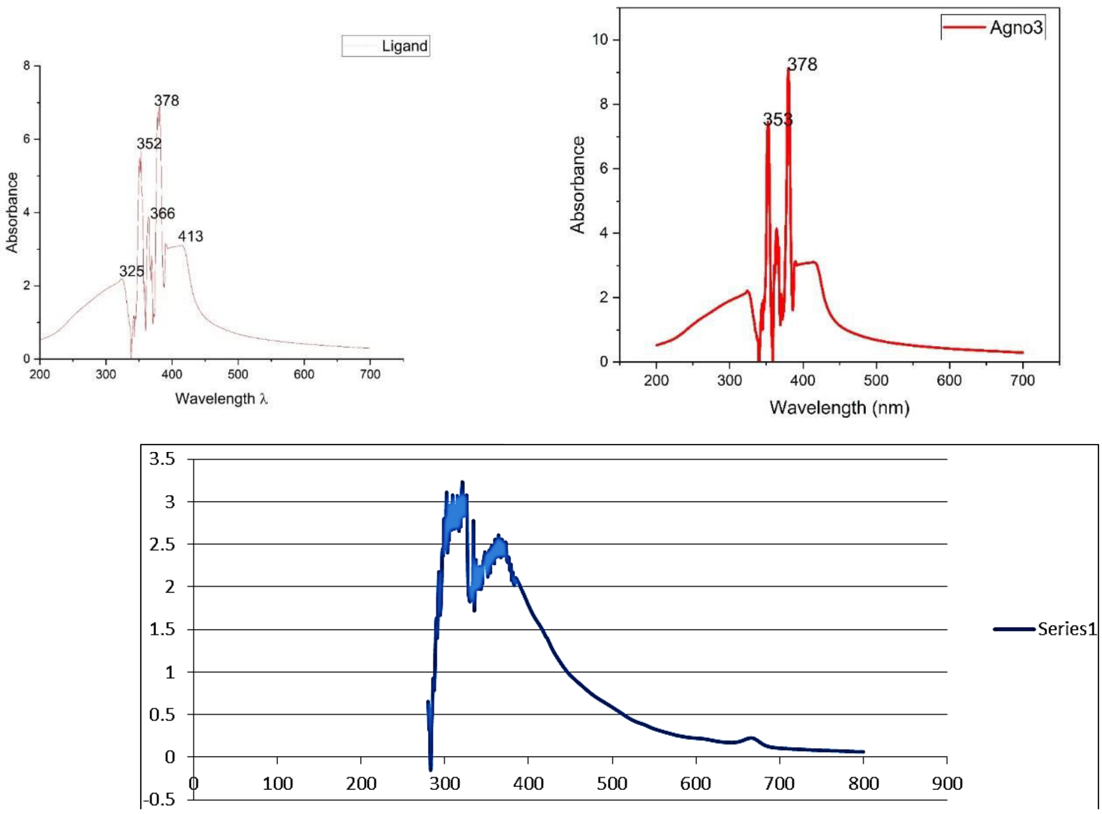

Figure -5 UV-Visible Spectra of ligand, Silver complex and silver nanoparticles

3.3.3 Proposed coordination Mode

Taken together, the FT-IR and UV-Vis spectroscopic data indicate a variable and asymmetric coordination environment in the silver complex. Coordination likely occurs via thiolate sulphur in silver complex, with additional involvement of the azomethine nitrogen in the complex. The lack of phenolic oxygen coordination is consistent across silver complex. These findings support the coordination modes in the spectra, highlighting distinct ligand -silver interactions dictated by structural features of the ligands.

3.3.4 X- ray diffraction studies

X -ray diffraction (XRD) is a critical crystallographic technique used to determine the crystalline nature of materials synthesised through both classical methods and modern approaches such as ultrasonication, biosynthesis and microwave -assisted synthesis.In this study,the structure & particle size of the synthesised compounds were characterized using a Bruker D8 Advance X- ray diffractometer. The measurements were conducted using CuKα radiation(λ=1.540A^0) with a 2θ range from 20 to 60^0.

Silver nanoparticles were obtained using synthesized silver (I) complex as a single molecular precursor, as evidenced by the x-ray diffraction (XRD) patterns shown in figure 6. Notably, the relatively high -intensity diffraction peaks at 64.4^0 and 77.3^0 indicate the presence of metallic silver, suggesting that the synthesis involving silver nanoparticles produced more elemental silver than other silver compounds. Figure –also includes standard reference patterns from the crystallography open Data base (Revision 204654, dated 2018/01/02), using the reference code 96-900-0254 for silver nano particles. Silver (I)complex successfully produced silver nanoparticles with average size of ≈78 nm. The average particle size was calculated using Debye- Scherrer equation:

D= K $\lambda/\beta COS\theta$

Where,

D= Average crystalline size

λ =x-ray wave length (1.540A^0)

$$\beta = Full\ width\ at\ half\ maximum\ (FWHM) of\ the\ diffraction\ peak (in\ radians$$

θ =Bragg angle

The broad and small reflections in the XRD patterns further further confirm the nanoscale size of the silver nano particles. The absence of additional peaks indicates that the nanoparticles synthesised using microwave assisted method are of high purity.The formation of nano crystalline, spherical silver nanoparticles is attributed to the green synthesis route employed.

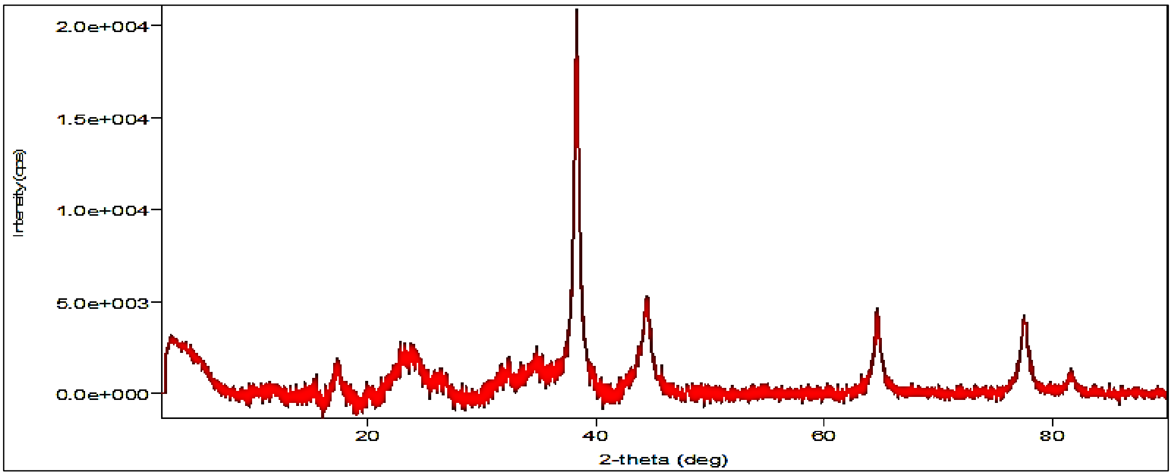

Figure -6 Powdered XRD of Microwave assisted Silver nanoparticles

3.3.5 Morphological Studies of Silver nanoparticles (TEM analysis)

The transmission electron micrograph (TEM) of silver nanoparticles synthesised from single molecular precursor of silver (I) complex is presented in figure-7. The image clearly reveals the formation of well-dispersed, predominantly spherical nanoparticles. The particle dimensions, including thickness and radius, were quantitatively estimated using Gatan Digital Micrograph software. The corresponding fast Fourier Transform (FFT) pattern as shown in figure.7, exhibits distinct and sharp diffraction spots, indicative of the high crystallinity of the synthesised silver nanoparticles. Furthermore, the well-defined lattice fringes observed in the high - resolution TEM(HRTEM) images confirm the crystalline nature at the atomic scale. The alternating dark & bright contrast of the fringes is consistent with the presence of periodic atomic arrangements, further validating the excellent crystalline quality of the silver nanoparticles. TEM images further revealed that the synthesised silver nanoparticles were well -dispersed and not agglomerated into clusters. The particles were separated by relatively uniform interparticle distances, indicating effective control over nucleation and growth processes. This spatial separation was clearly observed under high resolution TEM, supporting the formation of discrete, uniformly distributed nanoparticles with minimal aggregation.

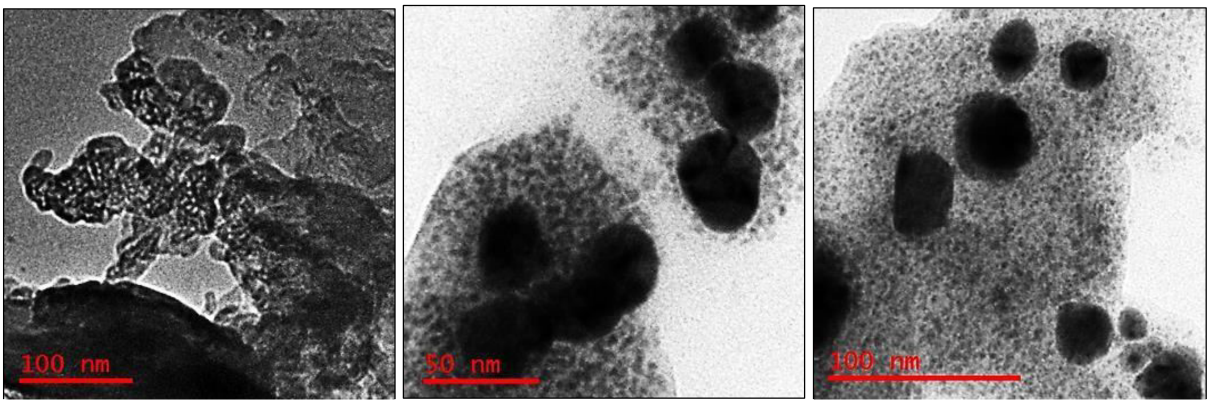

Figure 7– TEM Images of Microwave assisted silver nanoparticles derived from macrocyclic silver (I) complex

3.3.6 Energy -dispersive X-ray spectroscopy (EDX)-

EDX analysis of silver nanoparticles confirmed the presence of key constituent elements -carbon (C), nitrogen(N), sulphur (S) and silver (Ag) consistent with the proposed molecular structure of silver (I) complex. In addition, these elements, trace amount of chlorine (Cl) and calcium (Ca) were also detected. These are likely attributed to interactions with solvents during the refluxing and recrystallization steps employed for the purification of the complex prior to its use in the green synthesis of silver nanoparticles. TEM micrographs showed that silver nano particles were not accumulated in clusters but they were separated by equal space which was proved by microscopy visualizing under the high resolution microscope.

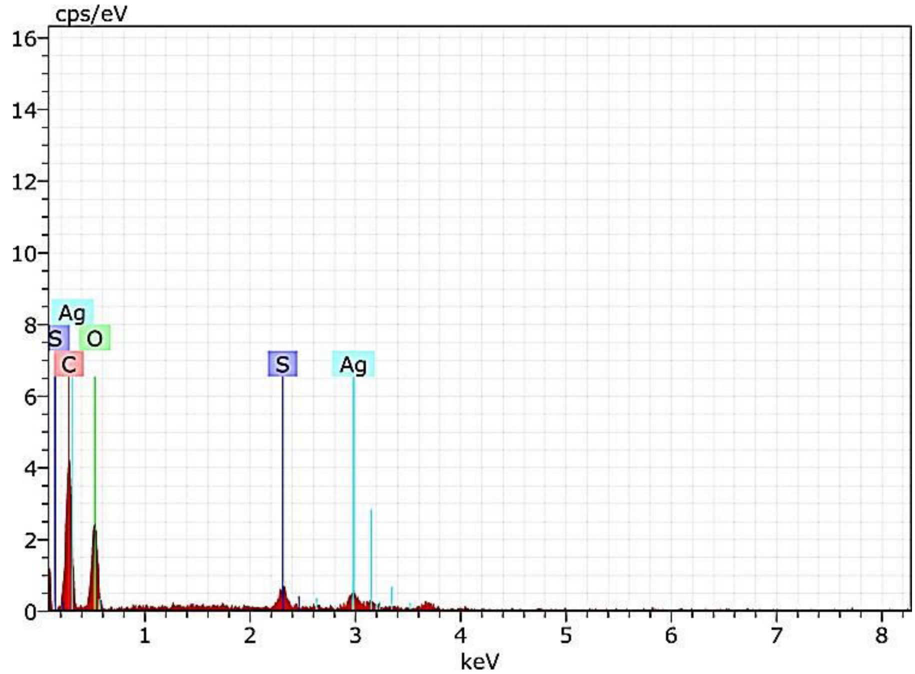

Figure –8 EDX Spectra of Microwave assisted Silver nanoparticles

3.3.7 Scanning Electron Microscopic analysis of silver nanoparticles-

Scanning Electron Microscopy (SEM) analysis was performed to examine the surface morphology and structural features of the green-synthesized silver nanoparticles. The SEM micrographs revealed that the nanoparticles were well-dispersed, exhibiting a versatile and predominantly oval-shaped morphology. These nanoparticles were synthesized by microwave irradiation of an ethanolic solution of the Ag(I) complex. Notably, the presence of ethanol as a solvent did not alter the morphology of the nanoparticles; however, it played a critical role in initiating the nucleation process, thereby facilitating the formation of silver nanoparticles. Furthermore, the SEM images demonstrated that the resulting silver nanoparticles were assembled into a loosely packed, quasi-linear arrangement, in contrast to the dense, closely packed configurations typically observed in conventional synthesis routes. This open structural assembly may have implications for enhanced surface area and potential functional applications in catalysis or sensing.

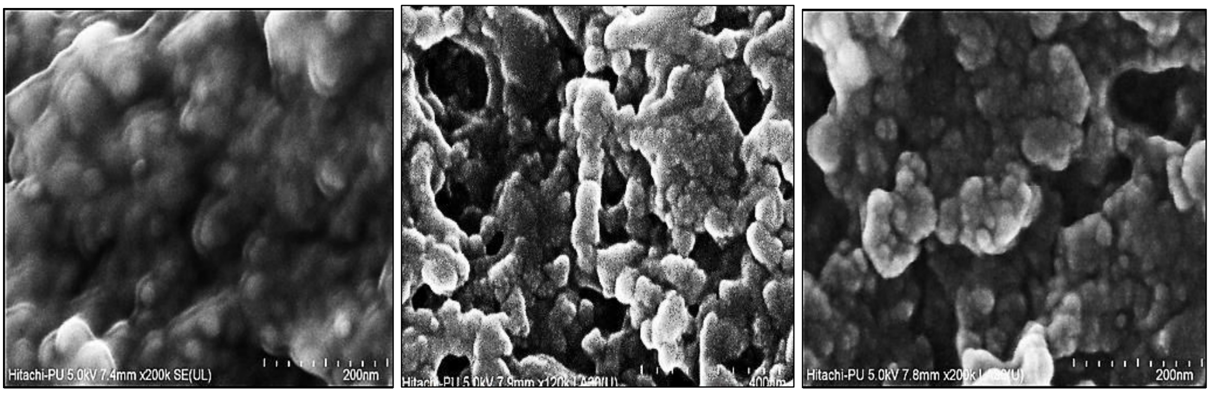

Figure -9 SEM micrographs of Microwave assisted silver nanoparticles

3.3.8 Thermogravimetric Analysis (TGA)

Thermogravimetric analysis (TGA) was performed to investigate the thermal stability and decomposition pattern of the synthesized silver (I) complex and its corresponding ligand. The TGA thermogram of the silver (I) complex shows distinct weight loss steps, initiating at 240.16 °C, followed by successive decomposition events at 251.21 °C and 279.30 °C, indicating a multi-step thermal degradation process. Comparative analysis of the decomposition profiles reveals that the silver (I) complex decomposes at significantly higher temperatures than its free ligand, suggesting enhanced thermal stability due to complexation. The TGA curve of the silver (I) complex exhibits a weight loss of 2.758 mg in the temperature range of 240–280 °C, corresponding to a calculated mass loss of 117.26%, which likely includes overlapping or consecutive decomposition events. In contrast, the TGA curve of the ligand displays multiple degradation steps with weight losses of 7.26 mg, 6.68 mg, and 7.36 mg, over corresponding temperature ranges, reflecting its lower thermal stability and stepwise breakdown. These results confirm that coordination with silver(I) imparts increased thermal resistance to the ligand, attributed to metal–ligand bonding interactions that stabilize the complex against thermal decomposition.

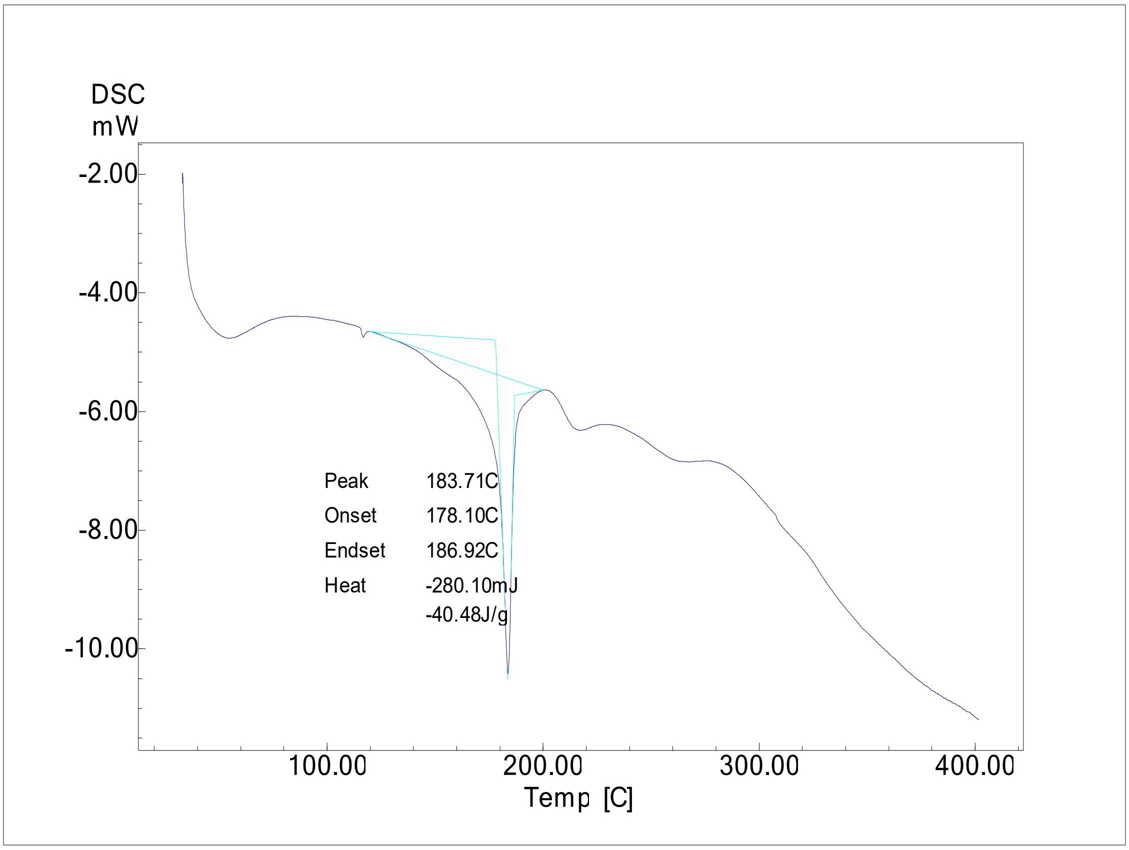

Figure – 10 TGA graph of Silver (I) complex

3.3.9 Antioxidant Activity via DPPH Radical Scavenging Assay

The antioxidant potential of the synthesized compounds was evaluated using the DPPH (2,2-diphenyl-1-picrylhydrazyl) radical scavenging assay, a well-established method for assessing free radical scavenging efficiency. The stable DPPH radical exhibits a characteristic deep violet colour, which undergoes a stoichiometric loss of colour upon reaction with a reducing agent or antioxidant. This decolorization is attributed to the pairing of electrons with the DPPH radical, and the degree of colour loss is directly proportional to the number of electrons accepted. The decrease in absorbance due to the reduction of DPPH radical3.3.9s by the test compound or standard (ascorbic acid) was measured spectrophotometrically using a UV-Visible spectrophotometer, and the results were used to calculate the IC_{50} values—the concentration required to inhibit 50% of the DPPH radicals.

It is well established that compounds exhibiting lower IC_{50} values are more potent free radical scavengers, indicating higher antioxidant potential. In the present study, the compound designated as Ag(I) complex demonstrated noteworthy antioxidant activity, confirming its ability to quench DPPH radicals. Among the tested compounds, the Ag(I) complex exhibited the lowest IC_{50} value of 54.24µg/mL, suggesting significant antioxidant activity. However, its activity was still slightly lower than that of the standard antioxidant ascorbic acid, which exhibited an IC_{50} value of 21.64 µg/mL under identical experimental conditions. These findings support the conclusion that both the Ag(I) complex possess appreciable antioxidant potential, with the Ag(I) complex showing relatively higher efficacy among the tested metal-based compounds.

Table 2. Percentage DPPH free radical inhibition activity by standard ascorbic acid at various concentrations.

S.No.	Concentration in µg/ ml	Absorption at 517nm	Percentage inhibition	IC_{50}
1.	0	0	0	21.63823
2.	20	0.552	42.01681	
3.	40	0.321	66.28151	
4.	60	0.225	76.36555	
5.	80	0.112	88.23529	
6.	100	0.098	89.70588	

Table 3. Percentage DPPH frees radical inhibition activity by Schiff base at various concentrations.

S.No.	**Concentration in µg/ ml**	**Absorption at 517nm**	**Percentage inhibition**	**IC_{50}**
1.	0	0	0	52.83
2.	20	0.568	30.88235	
3.	40	0.489	40.33613	
4.	60	0.325	48.63445	
5.	80	0.223	65.86134	
6.	100	0.658	76.57563	

Table 4. Percentage DPPH frees radical inhibition activity of Silver nanoparticles at various concentrations.

S.No.	**Concentration in µg/ ml**	**Absorption at 517nm**	**Percentage inhibition**	**IC_{50}**
1.	0	0	0	54.25
2.	20	0.573	32.882	
3.	40	0.492	43.3362	
4.	60	0.345	49.63446	
5.	80	0.253	68.86134	
6.	100	0.668	77.57683	

Mechanism of Antioxidant Activity of Synthesized Compounds

The antioxidant activity of the synthesized compounds was evaluated using the DPPH (2,2-diphenyl-1-picrylhydrazyl) radical scavenging assay. The DPPH molecule possesses an unpaired electron on the nitrogen atom, which is responsible for its characteristic absorbance at 517 nm and the appearance of a deep purple colour in solution. Upon interaction with an antioxidant, the DPPH radical accepts a hydrogen atom or an electron, resulting in a decrease in absorbance and a gradual fading of the purple coloration.

This decolorization reflects the scavenging capacity of the antioxidant compounds. The extent of the reaction can be quantitatively measured by monitoring the reduction in absorbance at 517 nm. To assess the reversibility of the reaction, DPPH-H is added at the end. An increase in the remaining percentage of DPPH radical at the plateau suggests a reversible reaction, while a lack of increase indicates a complete and irreversible reaction. The DPPH assay, therefore, provides a reliable estimate of the hydrogen-donating ability of a compound. Greater decolorization corresponds to higher antioxidant activity, which is expressed as a lower IC_{50} value. Thus, compounds with lower IC_{50} values are considered to have stronger free radical scavenging potential.

3.3.10 Anti-inflammatory Activity: Inhibition of Protein Denaturation

Protein denaturation is a biochemical process in which proteins lose their secondary and tertiary structures due to external stressors such as heat, acids, alkalis, organic solvents, or salts. This structural disruption often leads to a loss of biological function. Denatured proteins are known to act as inducers of inflammation, making protein denaturation assays a useful method for evaluating the anti-inflammatory potential of pharmacological agents.

In the present study, the anti-inflammatory activity of the synthesized ligand, its Silver(I) complex and silver nanoparticles was evaluated using the heat-induced albumin denaturation assay. The assay is based on the principle that agents capable of inhibiting thermally-induced protein denaturation possess anti-inflammatory properties.

The results demonstrated that the tested samples exhibited significant inhibition of albumin denaturation: The Silver(I) complex showed 65.9% inhibition at a concentration of 100 µg/mL .& silver sulphide nanoparticles showed 64.1% of inhibition at the same concentrations. In comparison, the standard anti-inflammatory drug Aspirin exhibited 70.7% inhibition at the same concentration. These findings suggest that the Silver(I) complex exhibits a comparable anti-inflammatory effect to Aspirin, thereby indicating its potential as an effective anti-inflammatory agent.

Table 5. Percentage inhibition of proteinase activity of Schiff base ligand against standard aspirin drug.

S.No.	**Compounds**	**Concentration in µg/ml**	**Absorption at 210 nm**	**Percentage inhibition**
1.	Control	100	0.733	0 %
2.	Aspirin	100	0.216	70.53 %
3.	Schiff base ligand	100	0.406	54 %
4.	Silver(I) Complex	100	0.706	65.9 %
5.	Silver sulphide nanoparticles	100	0.726	64.1 %

3.3.11 In Vitro Cytotoxic Activity of compounds

The cytotoxic potential of the synthesized ligand, its corresponding Ag(I) complex, and microwave-assisted silver sulphide nanoparticles was assessed against MCF-7 human breast cancer cell lines using the MTT assay (3-(4,5-dimethylthiazol-2-yl)-2,5-diphenyl tetrazolium bromide). The MCF-7 cells were procured from the National Centre for Cell Science (NCCS), Pune, and cultured under standard conditions. The assay evaluates mitochondrial activity as an indicator of cell viability, proliferation, and cytotoxicity. The cytotoxicity was tested across a concentration gradient (7.8–1000 µg/mL), with doxorubicin employed as the standard chemotherapeutic reference. The cell viability was inversely proportional to the concentration of the test compounds, confirming a dose-dependent cytotoxic response. Among the tested compounds, silver nanoparticles exhibited the highest cytotoxicity, followed by the Ag(I) complex, whereas the free ligand showed relatively lower activity. This enhanced cytotoxicity of the silver nanoparticles is attributed to their nanoscale dimensions, increased surface area, and efficient cellular internalization, which enhances interaction with intracellular targets and facilitates reactive oxygen species (ROS) generation, leading to cellular apoptosis. Additionally, the coordination of silver with the curcumin-based ligand improves bioavailability and stability, further amplifying anticancer potential. These results are in agreement with previous reports indicating the non-toxic and biocompatible nature of Ag NPs, and their promising applicability in targeted cancer therapy and diagnostics.[28]

Table -6 **In Vitro Cytotoxic Activity of Silver complex derived from macrocyclic ligand & microwave -assisted silver nanoparticles**

Test substance	**Concentratio non (µg/ml)**	**% of viability after treatment (Mean ± SD)**	**% of cell cytotoxicity after treatment (Mean ± SD)**	**CTC_{50}**
Silver (I) complex	**1000**	11.65 ± 0.51	88.35 ± 0.51	487.56±2.42
	500	24.31 ± 1.80	75.69 ± 1.80	
	250	38.73 ± 2.67	61.27 ± 2.67	
	125	68.35 ± 3.26	31.65 ± 3.26	
	62.5	81.87 ± 2.79	18.13 ± 2.79	
	31.25	89.89 ± 2.64	10.11 ± 2.64	
	15.625	95.32 ± 2.54	4.68 ± 2.54	
	7.8	98.54 ± 1.63	1.46 ± 1.63	
Silver nanoparticles	**1000**	11.75 ± 0.51	89.35 ± 0.51	248±2.66
	500	25.31 ± 1.80	76.69 ± 1.80	
	250	39.73 ± 2.67	62.27 ± 2.67	

	125	69.35 ± 3.26	32.65 ± 3.26	
	62.5	83.87 ± 2.79	19.13 ± 2.79	
	31.25	90.89 ± 2.64	12.11 ± 2.64	
	15.625	96.32 ± 2.54	4.69 ± 2.54	
	7.8	98.54 ± 1.63	1.49 ± 1.63	1.46 ± 1.63
	1000	47.65 ± 0.51	52.35 ± 0.51	
	500	66.31 ± 1.80	33.69 ± 1.80	
	250	78.73 ± 2.67	21.27 ± 2.67	
	125	82.35 ± 3.26	17.65 ± 3.26	853.98±2.68
	62.5	90.87 ± 2.79	9.13 ± 2.79	
	31.25	95.89 ± 2.64	4.11 ± 2.64	
	15.625	97.32 ± 2.54	2.68 ± 2.54	
	7.8	99.54 ± 1.63	0.46 ± 1.63	

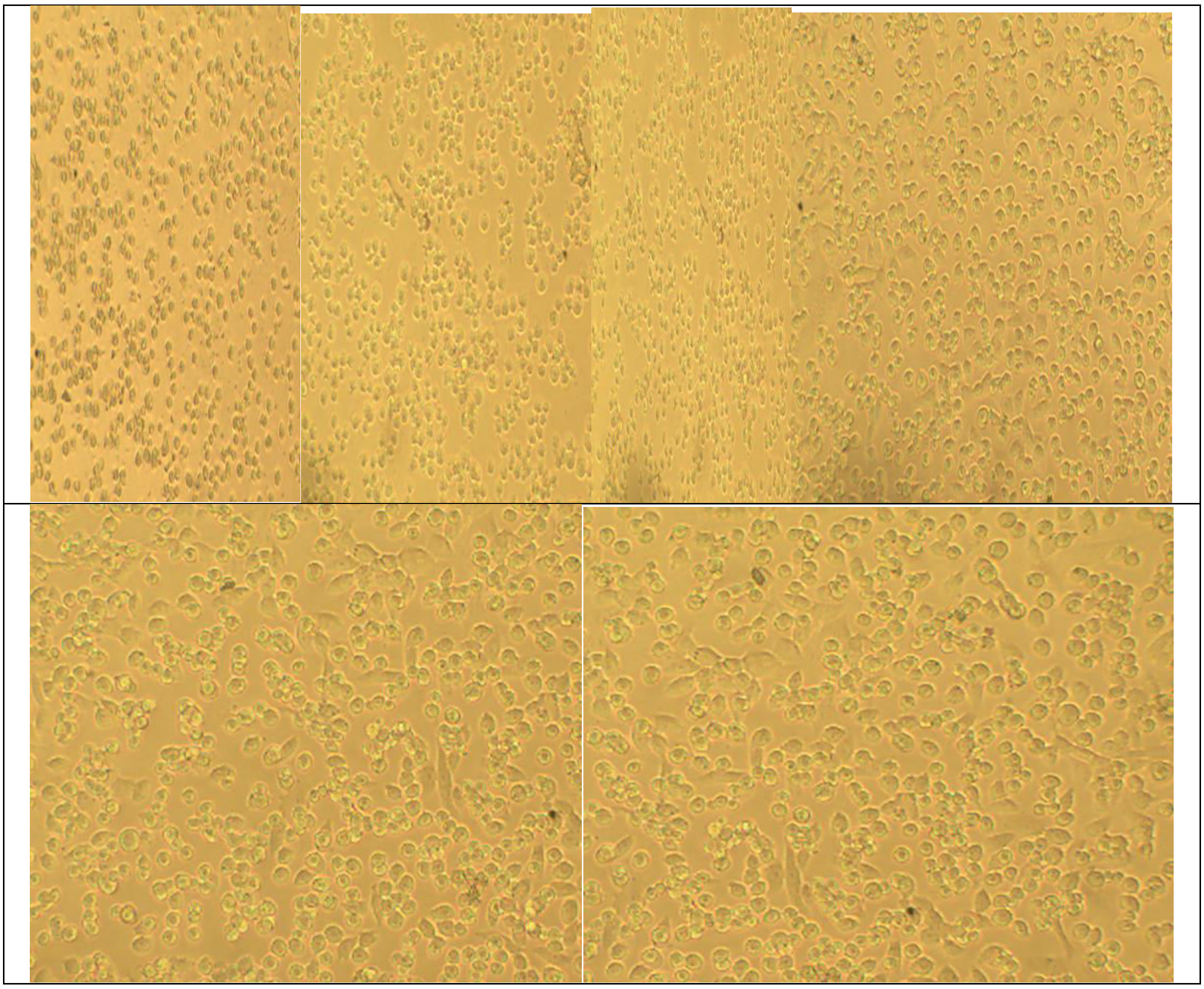

Figure -11 Anticancer activities of ligand, Silver (I) complex & Microwave assisted Silver nanoparticles

4. CONCLUSION

Highly biologically active Ag NPs were successfully synthesized via an eco-friendly microwave-assisted method using a silver(I) complex derived from a Schiff base ligand formed by the condensation of curcumin and thiosemicarbazide hydrochloride. This rapid and green synthesis approach utilizes microwave irradiation to efficiently decompose the Ag(I) complex, yielding well-defined spherical silver nanoparticles within a remarkably short reaction time. Morphological and structural characterizations confirmed that the size and shape of the resulting silver nanoparticles are significantly influenced by the concentration of the Ag(I) precursor complex. The microwave irradiation not only enhances the rate of decomposition of the silver complex but also minimizes side reactions, promoting the formation of uniform, fine-quality nanoparticles with consistent morphology. This method is simple, cost-effective, time-efficient, and environmentally sustainable, making it highly suitable for scaling up to industrial-level production of silver nanoparticles. Moreover, the biological evaluation of the synthesized silver nanoparticles revealed promising results, indicating potential applications in pharmaceutical and biomedical domains. Specifically, the AgNP's exhibited notable antibacterial, antioxidant, and anti-inflammatory activities, highlighting their promise as a multifunctional drug candidate for future therapeutic applications.

5. ACKNOWLEDGEMENT

The authors sincerely acknowledge the Madhya Pradesh Council of Science and Technology (MPCST), Bhopal, for the financial support provided through a research grant (Dated 31/03/2023, File No. A/RD/RP-2/347). The authors are also grateful to the Department of Chemistry, School of Sciences, ITM University, Gwalior (M.P.), for extending laboratory infrastructure and research facilities essential for this work. Special appreciation is extended to the Central Instrumentation Facility (CIF), Jiwaji University, Gwalior, and the Spectroscopy and Instrumentation Facility (SIF), ITM University, for their technical assistance in spectral data acquisition and analytical support. The authors also wish to thank Radiant Research Lab, Bangalore, for their valuable contribution to the biological evaluation studies of the synthesized compounds.

REFERENCES

[1] Gurunathan, S.; Park, J.H.; Han, J.W.; Kim, J.H. Comparative assessment of the apoptotic potential of silver nanoparticles synthesized by *Bacillus tequilensis* and *Calocybe indica* in MDA-MB-231 human breast cancer cells: Targeting p53 for anticancer therapy. *Int. J. Nanomed.* **2015**, *10*, 4203–4222.

[2] Li, W.R.; Xie, X.B.; Shi, Q.S.; Zeng, H.Y.; Ou-Yang, Y.S.; Chen, Y.B. Antibacterial activity and mechanism of silver nanoparticles on *Escherichia coli*. *Appl. Microbiol. Biotechnol.* **2010**, *8*, 1115–1122.

[3] Mukherjee, P.; Ahmad, A.; Mandal, D.; Senapati, S.; Sainkar, S.R.; Khan, M.I.; Renu, P.; Ajaykumar, P.V.; Alam, M.; Kumar, R.; et al. Fungus-mediated synthesis of silver nanoparticles and their immobilization in the mycelial matrix: A novel biological approach to nanoparticle synthesis. *Nano Lett.* **2001**, *1*, 515–519.

[4] Chernousova, S.; Epple, M. Silver as antibacterial agent: Ion, nanoparticle, and metal. *Angew. Chem. Int. Ed.* **2013**, *52*, 1636–1653.

[5] Li, C.Y.; Zhang, Y.J.; Wang, M.; Zhang, Y.; Chen, G.; Li, L.; Wu, D.; Wang, Q. In vivo real-time visualization of tissue blood flow and angiogenesis using Ag_2S quantum dots in the NIR-II window. *Biomaterials* **2014**, *35*, 393–400

[6] Sondi, I.; Salopek-Sondi, B. Silver nanoparticles as antimicrobial agent: A case study on *E. coli* as a model for Gram-negative bacteria. *J. Colloid Interface Sci.* **2004**, *275*, 177–182.

[7] Li, L.; Hu, J.; Yang, W.; Alivisatos, A.P. Band gap variation of size- and shape-controlled colloidal CdSe quantum rods. *Nano Lett.* **2001**, *1*, 349–351.

[8] Sharma, V.K.; Yngard, R.A.; Lin, Y. Silver nanoparticles: Green synthesis and their antimicrobial activities. *Adv. Colloid Interface* **2009**, *145*, 83–96

[9] Gurunathan, S.; Kalishwaralal, K.; Vaidyanathan, R.; Venkataraman, D.; Pandian, S.R.; Muniyandi, J.; Hariharan, N.; Eom, S.H. Biosynthesis, purification and characterization of silver nanoparticles using *Escherichia coli*. *Colloids Surf. B Biointerfaces* **2009**, *74*, 328–335.

[10] Lin, P.C.; Lin, S.; Wang, P.C.; Sridhar, R. Techniques for physicochemical characterization of nanomaterials. *Biotechnol. Adv.* **2014**, *32*, 711–726.

[11] Pleus, R. *Nanotechnologies-Guidance on Physicochemical Characterization of Engineered Nanoscale Materials for Toxicologic Assessment*; ISO: Geneva, Switzerland, 2012.

[12] Murdock, R.C.; Braydich-Stolle, L.; Schrand, A.M.; Schlager, J.J.; Hussain, S.M. Characterization of nanomaterial dispersion in solution prior to in vitro exposure using dynamic light scattering technique. *Toxicol. Sci.* **2008**, *101*, 239–253.

[13] Gurunathan, S.; Han, J.W.; Kim, E.S.; Park, J.H.; Kim, J.H. Reduction of graphene oxide by resveratrol: A novel and simple biological method for the synthesis of an effective anticancer nanotherapeutic molecule. *Int. J. Nanomed.* **2015**, *10*, 2951–2969.

[14] Sapsford, K.E.; Tyner, K.M.; Dair, B.J.; Deschamps, J.R.; Medintz, I.L. Analyzing nanomaterial bioconjugates: A review of current and emerging purification and characterization techniques. *Anal. Chem.* **2011**, *83*, 4453–4488.

[15] Carlson, C.; Hussain, S.M.; Schrand, A.M.; Braydich-Stolle, L.K.; Hess, K.L.; Jones, R.L.; Schlager, J.J. Unique cellular interaction of silver nanoparticles: Size-dependent generation of reactive oxygen species. *J. Phys. Chem. B* **2008**, *112*, 13608–13619.

[16] Jo, D.H.; Kim, J.H.; Lee, T.G.; Kim, J.H. Size, surface charge, and shape determine therapeutic effects of nanoparticles on brain and retinal diseases. *Nanomedicine* **2015**, *11*, 1603–1611.

[17] Dhanorya, D., Pnadey, V., Shukla, R., Vishwakarma, Y., Bairagi, G. K., Gupta, V., ... & Anand, S. (2025). A Comprehensive Review on Medicinal Herbal Plant with Potential Hypolipidemic Activity. *Pharmacognosy Research*, *17*(2).

[18] Anand, S., Bajhaiya, M. K., Singh, S., Sharma, A., Kumar, L., Kumar, D., ... & Raj, D. (2024). ROLE/ASSOCIATION OF MTHFR GENE WITH DOWNS SYNDROME.

[19] Albanese, A.; Tang, P.S.; Chan, W.C. The effect of nanoparticle size, shape, and surface chemistry on biological systems. *Annu. Rev. Biomed. Eng.* **2012**, *14*, 1–16.

[20] Panáček, A.; Kolář, M.; Večeřová, R.; Prucek, R.; Soukupová, J.; Kryštof, V.; Hamal, P.; Zbořil, R.; Kvítek, L. Antifungal activity of silver nanoparticles against Candida spp. *Biomaterials* **2009**, *30*, 6333–6340.

[21] Zodrow, K.; Brunet, L.; Mahendra, S.; Li, D.; Zhang, A.; Li, Q.; Alvarez, P.J. Polysulfone ultrafiltration membranes impregnated with silver nanoparticles show improved biofouling resistance and virus removal. *Water Res.* **2009**, *43*, 715–723.

[22] Wong, K.K.; Cheung, S.O.; Huang, L.; Niu, J.; Tao, C.; Ho, C.M.; Che, C.M.; Tam, P.K. Further evidence of the anti-inflammatory effects of silver nanoparticles. *ChemMedChem* **2009**, *4*, 1129–1135.

[23] Gurunathan, S.; Lee, K.J.; Kalishwaralal, K.; Sheikpranbabu, S.; Vaidyanathan, R.; Eom, S.H. Antiangiogenic properties of silver nanoparticles. *Biomaterials* **2009**, *30*, 6341–6350.

[24] Anand, S., kumar Bajhaiya, M., Singh, S., Sharma, A., Patel, H. S., Raj, H., & Raj, D. (2024). Antiviral Flavonoids as a Potential Substitute for Overcoming Antiviral Resistance. *Asian Journal of Basic Science & Research*, *6*(4), 49-61.

[25] American Cancer Society. *Cancer Facts & Figures 2015*; American Cancer Society: Atlanta, GA, USA, 2015.

[26] W.J. Geary. The Use of Conductivity Measurements in Organic Solvents for the Characterisation of Coordination Compounds. *Coordination Chemistry Reviews* **7** (1971) 81-122. http://dx.doi.org/10.1016/S0010-8545(00)80009-0.

[27] C.W. Lange, C.G. Pierpont. Nickel complexes containing catecholate, benzoquinone and semiquinone radical ligands. *Inorganica Chimica Acta* **263** (1997) 219-224. https://doi.org/10.1016/S0020-1693(97)05649-1.

[28] F. Scholz, Electroanalytical Methods: Guide to Experiments and Applications, 1st ed. SpringerVerlag, Berlin, Germany, 2002, p. 331